## Journal Pre-proof

Significant phase-space-driven thermal transport suppression in BC8 silicon

Junyan Liu, Timothy A. Strobel, H. Zhang, Doug Abernathy, Chen Li, Jiawang Hong

PII: S2542-5293(21)00227-3

DOI: https://doi.org/10.1016/j.mtphys.2021.100566

Reference: MTPHYS 100566

To appear in: Materials Today Physics

Received Date: 22 September 2021

Revised Date: 25 October 2021 Accepted Date: 27 October 2021

Please cite this article as: J. Liu, T.A. Strobel, H. Zhang, D. Abernathy, C. Li, J. Hong, Significant phase-space-driven thermal transport suppression in BC8 silicon, *Materials Today Physics*, https://doi.org/10.1016/j.mtphys.2021.100566.

This is a PDF file of an article that has undergone enhancements after acceptance, such as the addition of a cover page and metadata, and formatting for readability, but it is not yet the definitive version of record. This version will undergo additional copyediting, typesetting and review before it is published in its final form, but we are providing this version to give early visibility of the article. Please note that, during the production process, errors may be discovered which could affect the content, and all legal disclaimers that apply to the journal pertain.

© 2021 Elsevier Ltd. All rights reserved.



## Journal Pre-proof

#### **Author contributions**

Junyan Liu: Calculation; Writing the original manuscript; Writing - review & editing;

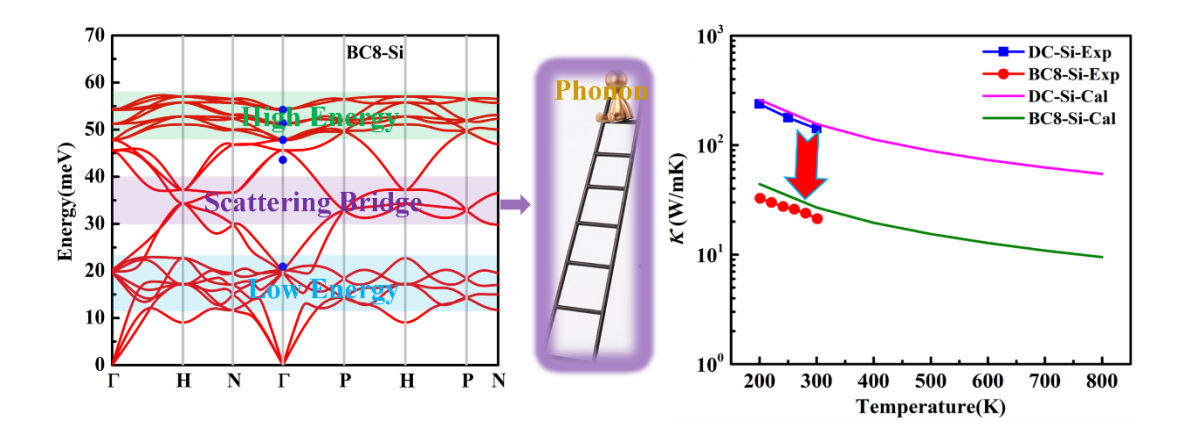
**Timothy A. Strobel**: Neutron inelastic scattering measurement; Reviewing the manuscript;

H. Zhang: Preparing and providing samples; Neutron inelastic scattering measurement;

Doug Abernathy: Reviewing the manuscript;

**Chen Li**: Guiding the experiments; Funding acquisition; Writing - review & editting; Project administration Supervis.

**Jiawang Hong**: Guiding the calculations; Funding acquisition; Writing - review & edittting; Project administration Supervis.



Significant phase-space-driven thermal transport suppression in

**BC8** silicon

Junyan Liu<sup>1</sup>, Timothy A. Strobel<sup>2</sup>, H. Zhang<sup>2</sup>, Doug Abernathy<sup>3</sup>, Chen Li<sup>4,5</sup>\*, Jiawang Hong<sup>1</sup>\*

<sup>1</sup>School of Aerospace Engineering, Beijing Institute of Technology, Beijing, 100081, China

<sup>2</sup>Carnegie Institution for Science, Earth and Planets Laboratory, Washington, DC 20015, USA

<sup>3</sup>Neutron Scattering Division, Oak Ridge National Laboratory, Oak Ridge, TN 37830, USA

<sup>4</sup>Department of Mechanical Engineering, University of California, Riverside, CA 92521, USA

<sup>5</sup>Materials Science and Engineering, University of California, Riverside, CA 92521, USA

Corresponding Author

\*E-mail: hongjw@bit.edu.cn; chenli@ucr.edu

**Abstract:** The BC8 silicon allotrope has a lattice thermal conductivity 1-2 orders of magnitude

lower than that of diamond-cubic silicon. In the current work, the phonon density of states,

phonon dispersion, and lattice thermal conductivity are investigated by inelastic neutron

scattering measurements and first-principles calculations. Flat phonon bands are found to play

a critical role in the reduction of lattice thermal conductivity in BC8-Si. Such bands in the low-

energy range enhance the phonon scattering between acoustic and low-energy optical phonons,

while bands in the intermediate-energy range act as a scattering bridge between the high- and

low-energy optical phonons. They significantly enlarge the phonon-phonon scattering phase

space and reduces the lattice thermal conductivity in this novel silicon allotrope. This work

provides insights into the significant reduction of the lattice thermal conductivity in BC8-Si,

thus expanding the understanding of novel silicon allotropes and their development for

electronic devices.

**Keywords** 

Silicon allotrope, Lattice thermal conductivity, Inelastic neutron scattering measurements,

First-principles calculations

1

#### 1. Introduction

With the development of novel synthesis techniques[1] including extreme synthesis conditions[2,3], numerous silicon allotropes were discovered in recent years, including Si-II[4], Si-V[5], Si-VI[6], Si-VII[5], Si-VIII[7], Si-X[8], Si-XI[9,10], Si-XIII[11], etc. Among them, Si-III (BC8-Si)[12], Si-IV (HD-Si)[11], Si-XII (R8-Si)[13,14], zeolite types Si<sub>136</sub>,[15] and Si<sub>24</sub>, [2] are recoverable phases that remain metastable at ambient conditions. Many of these allotropes have novel properties beyond those of diamond-cubic silicon (DC-Si). For example, Si<sub>24</sub>,[2] and tI16-Si[16] have a quasi-direct band gap near 1.4 eV and a direct band gap of 1.25 eV, respectively, which is close to the optimum value for solar conversion, while maintaining large carrier mobility and low mass density[17]. Additionally, the thermal conductivity of Si<sub>24</sub> is 1/13<sup>th</sup> that of DC-Si[18], suggesting promise in thermoelectric applications. While several new silicon allotropes[19,20] with novel electronic properties[17] have been investigated, experimental studies of thermal transport properties are rare, mainly due to the small sample sizes limited by high-pressure synthesis.

Recently, large and phase-pure samples of BC8-Si (*cI*16) were successfully synthesized by the multi-anvil press method[12], opening the possibility for novel measurements. BC8-Si is a narrow-gap semiconductor with an electrical conductivity of 76 S/cm at 300 K thanks to its high carrier density. Moreover, a recent study revealed that BC8-Si has a remarkably low thermal conductivity: 1-2 orders of magnitude lower than that of DC-Si depending on the temperature. This result appears highly unusual since BC8-Si and DC-Si both have cubic structures[20]. The microscopic origin of this thermal transport difference is still unclear due to the lack of knowledge on the lattice dynamics of BC8-Si.

In this work, the primary origin of the strikingly different thermal conductivities of BC8-Si and DC-Si is revealed by combining inelastic neutron scattering (INS) measurements and first-principles simulations. INS experiments were performed on DC- and BC8-Si samples to obtain the phonon density of states (DOS) at ambient temperature and the results reveal softer phonons in BC8-Si. The first-principles simulations indicate that the reduction of lattice thermal conductivity in BC8-Si mainly results from the enlarged phonon-phonon scattering phase space induced by flat phonon bands, which act as a bridge between low-energy and high-energy optic branches. The results offer microscopic insights into thermal transport in BC8-Si

and further exploration of the thermal properties of silicon allotropes.

## 2. Experimental and Computational Methods

Bulk samples of BC8-Si used for the INS measurements were synthesized via direct transformation of elemental silicon using the multi-anvil press method[12]. The recovered samples were determined to be homogeneous and phase-pure through characterization using X-ray diffraction, Raman spectroscopy, and nuclear magnetic resonance spectroscopy[21]. A total sample mass of 10 milligrams of BC8-Si was used for INS and 5 grams of crystalline DC-Si sample was used for comparison.

INS measurements were performed on the Wide Angular-Range Chopper Spectrometer (ARCS), a direct geometry chopper neutron spectrometer at Oak Ridge National Laboratory. Both samples were sealed with thin aluminum foil and loaded on a sample stick without sample environment to minimize the measurement background. All measurements were performed at ambient temperature (295 K). ARCS has an energy resolution of 1.4-3 meV[22] for the neutron incident energy ( $E_i$ ) of 40 and 75 meV chosen to optimize the energy resolution and range (Fig. 1).

MANTID software[23] was used for the data reduction. The event mode data of ARCS measurement contains the information of the detector number and the time-of-arrival of each scattered neutron. The momentum (q) and energy transfer of scattered neutrons were calculated from their time-of-flight and scattering geometry to generate the dynamical structure factor, S(q, E). Measurements on an empty instrument suggest that the background is negligible, so the background subtraction is not needed. The phonon spectra were calculated based on the incoherent approximation, which has been shown to work reliably[24,25]. Elastic intensities were removed below 5 meV and the phonon DOS below this cutoff was extrapolated by the Debye model. The energy bin sizes were set at 0.5 and 1 meV for  $E_i = 40$  and 75 meV, respectively. Due to the small sample thickness, no multiple scattering correction was necessary[24]. The phonon spectra were also corrected for the Boltzmann factor.

First-principles calculations based on the density-functional theory (DFT) were performed using the projector-augmented wave (PAW) method[26] as implemented in the Vienna Ab Initio Simulation (VASP) Package[27]. The generalized gradient approximation (GGA) of Perdew-Burke-Ernzerhof (PBE) for the exchange-correlation functional[28] was

used. The cut-off energy of plane wave basis was set 500 eV and the first Brillouin zone of the reciprocal space was sampled with Monkhorst-Pack[29] *k*-point meshes of 12×12×12 for DC-Si and 15×15×15 for BC8-Si. Two structures were fully relaxed until the force on each atom is smaller than 0.001 eV/Å and the optimized lattice constants are 5.469 and 6.622 Å for DC-Si and BC8-Si, respectively. The Phonopy package[30] and the ShengBTE code[31] based on the Boltzmann transport theory were used to obtain phonon dispersion and thermal conductivity, respectively.

## 3. Results and discussions

The phonon DOS of DC-Si and BC8-Si measured by INS, as shown in Fig.1a, and b, are in qualitative agreement with the first-principles simulation results. The experimental phonon population is the largest around 40 meV in BC8-Si, while the phonon population of DC-Si is low in the middle energy region. Compared with DC-Si, the phonon spectrum is softer (lower in energy) in BC8-Si for the features below 25 meV and above 50meV. The effects of these differences on thermal transport property of BC8-Si are worth investigation.

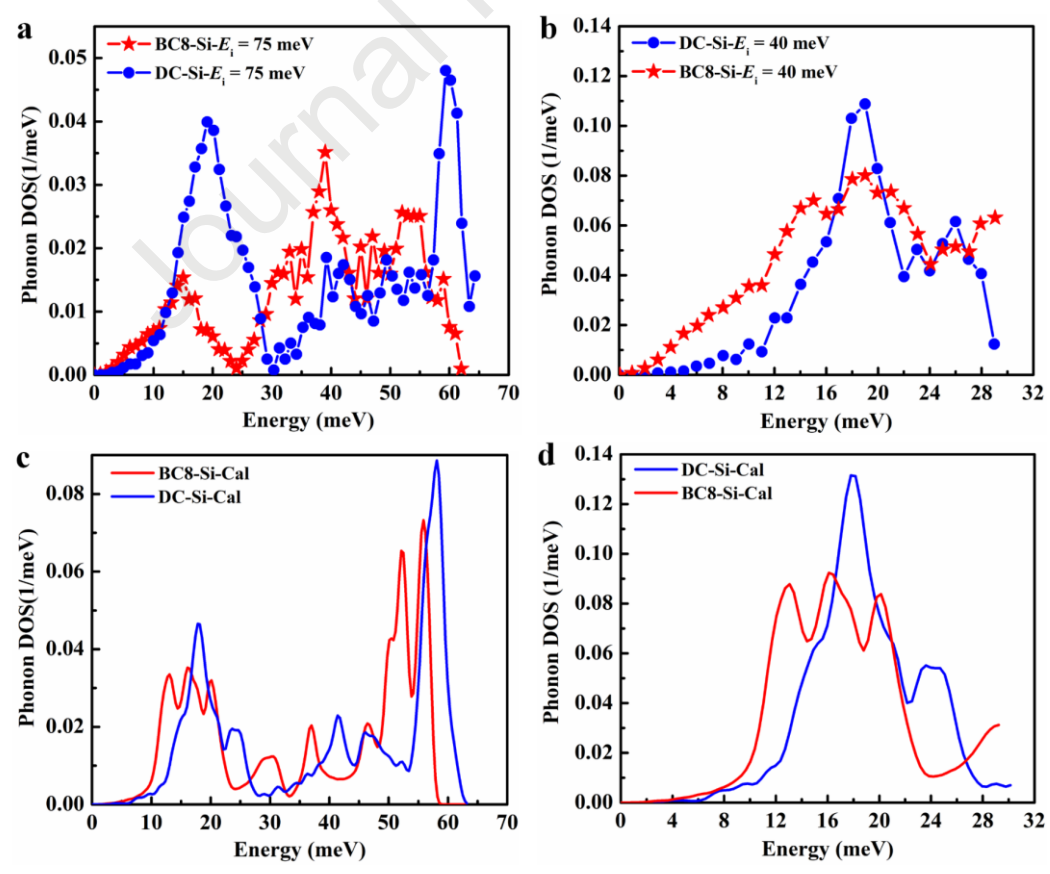


**Fig. 1.** The phonon density of states of DC-Si and BC8-Si measured by INS with incident energies of (a) 75 and (b) 40 meV at 295 K show significant difference. The first-principles

simulation is plotted in the same energy ranges for comparison (c) (d).

The phonon dispersions of the two materials along the high-symmetry directions of the Brillouin zone are plotted in Fig.2a,b. Measured phonon dispersion of DC-Si from INS[32] and Γ-point phonon energy of BC8-Si from Raman spectrascopy[21] are in good agreement with our first-principles calculations. Compared with DC-Si, the number of phonon branches of BC8-Si quadrupled because of the larger primitive cell. This will enhance the phonon scattering in BC8-Si and reduce its lattice thermal conductivity[33]. The overall phonon energy of BC8-Si is softer, and this is consistent with the phonon DOS in Fig.1. The low-energy optic phonon branches in BC8-Si cross with the acoustic phonon branches and form a series of non-dispersive, "flat" bands between 10 and 20 meV, while the high-energy optic phonons show flat bands spaced at equal energy intervals. In addition, between 30 and 40 meV, there are a few "flat" optical phonon branches in BC8-Si, corresponding to the peaks in its PDOS (Fig.1).

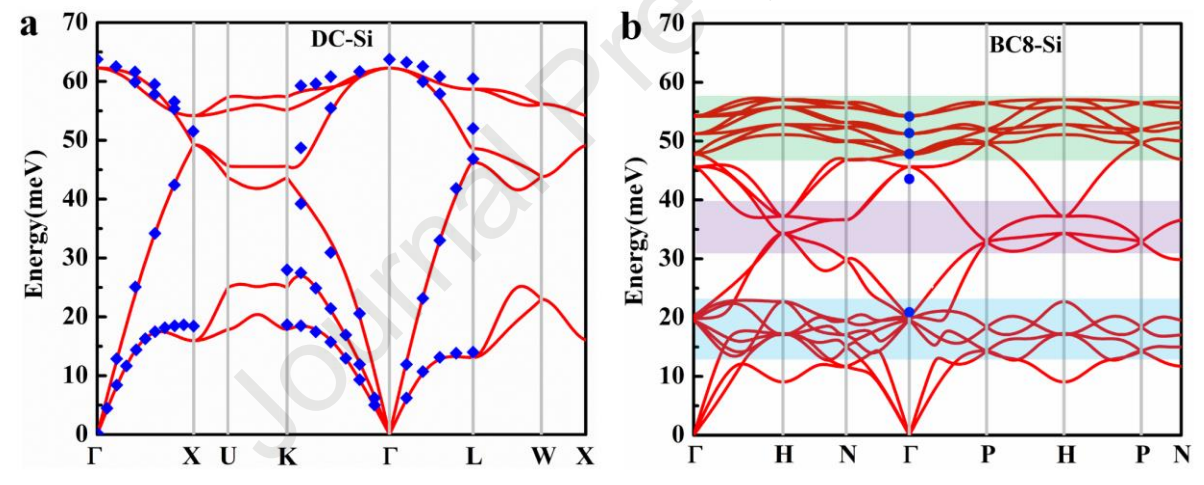


**Fig. 2.** Phonon dispersion of (a) DC-Si and (b) BC8-Si from first-principles calculations. The blue diamonds in (a) are INS results from Ref. 32 and the blue dots at  $\Gamma$  point in (b) are Raman results from Ref. 21.

The calculated temperature-dependent lattice thermal conductivity for DC-Si and BC8-Si agree well with available experiment values[12], as shown in Fig. 3a. The slight overestimation is because phonon scattering by boundaries, defects, etc. are not considered. The lattice thermal conductivity of BC8-Si (26.96 W/(m·K)) is about one sixth of that of DC-Si (155.80 W/(m·K)) at 300 K, reproducing well the trend of available experimental results from 200 to 300 K.

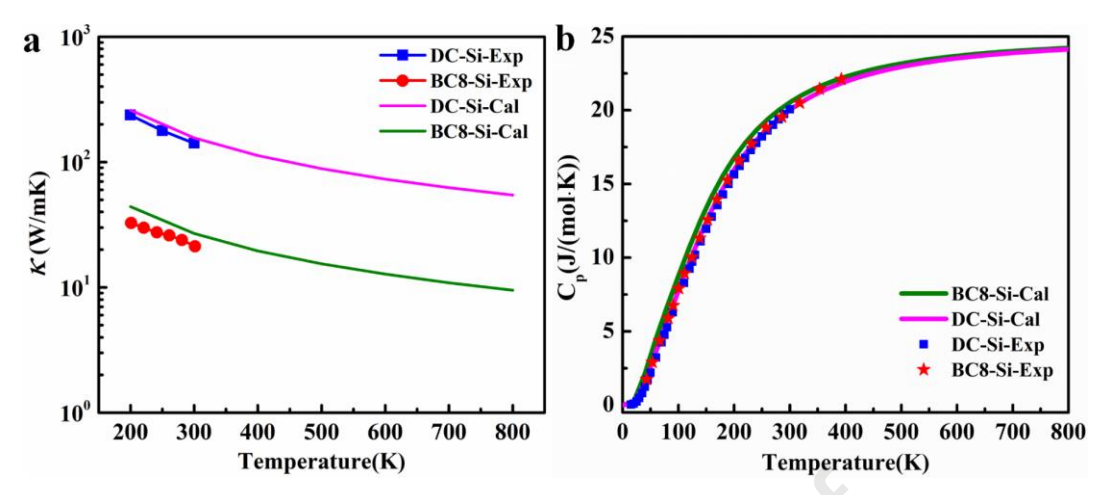


**Fig. 3.** Temperature dependence of (a) lattice thermal conductivity, (b) the heat capacity from calculation and experiment for DC-Si and BC8-Si. The experimental results are from Ref.12.

To reveal the origin of such remarkable differences in lattice thermal conductivity between BC8-Si and DC-Si, the lattice thermal conductivity is decomposed into three main factors for investigation, i.e., the heat capacity,  $c_{qj}$ , group velocity,  $v_{qj}$ , and phonon lifetime,  $\tau_{qj}$  (of wave vector  $\mathbf{q}$  and branch index j) in Eq.(1)[34].

$$\kappa = \frac{1}{3} \sum_{qj} c_{qj} v_{qj}^2 \tau_{qj}. \tag{1}$$

Firstly, the lattice heat capacity of DC-Si and BC8-Si is calculated and compared with available experimental results, as shown in Fig.3b. Both the experimental and computational lattice heat capacity of DC-Si are very close to that of BC8-Si (Fig. 3b), indicating that the lattice heat capacity contributes little to the large difference of thermal conductivity between the two phases. Secondly, to evaluate the role of the group velocity, the acoustic phonon group velocities are extracted from the phonon dispersion, as listed in Table I. The group velocity of the longitudinal acoustic (LA) mode and the transverse acoustic TA2 mode of BC8-Si are only slightly lower (~5%) along [010] directions when compared with those of DC-Si. On the other hand, the group velocity of the transverse acoustic mode TA1 is much larger in DC-Si. The group velocity of acoustic TA1 mode of BC8-Si does not explain its much lower lattice thermal conductivity even with a 41% smaller group velocity.

**Table I**. Group velocity ( $v_g$ , unit in m/s) of LA, TA<sub>1</sub> and TA<sub>2</sub> modes along the [010] directions.

	$v_{ m LA}$	<i>v</i> <sub>TA2</sub>	v tai
DC-Si	8323	5525	5525
BC8-Si	7971	5238	3240
$(v_{ m BC8}$ - $v_{ m DC})\!/v_{ m DC}$	-4%	-5%	-41%

As the heat capacity and the group velocity are ruled out as the main source for the large difference in thermal conductivity, the effects from phonon lifetime are analyzed. As shown in Fig.4a, the phonon-phonon scattering rates in BC8-Si are larger than that of DC-Si over the entire energy range, especially between 20 and 40 meV, suggesting that the shorter phonon lifetime is the main reason for the lower lattice thermal conductivity of BC8-Si. The phonon scattering rates depend on the phonon-phonon scattering phase-space and scattering probability determined by the third-order force constants ( $\Phi^{(3)}$ ). Fig.4c displays the Grüneisen parameter, which is usually used to approximately characterize the magnitude of  $\Phi^{(3)}$ . Because no major difference is found between the Grüneisen parameters of the two samples (Fig. 4d), the phonon scattering space weighted by the phonon occupation factor[35] are calculated (Fig. 4b). It turns out that the total weighted phase space of BC8-Si is about one order of magnitude greater than that of DC-Si. This enlarged scattering space in BC8-Si originates predominantly from its phonon dispersion, as shown in Fig.4c for different types of three-phonon scattering processes. The phonon-phonon scattering mostly occurs in acoustic phonons for DC-Si, while the optical phonons are much more involved in the phonon scattering processes in BC8-Si. The dimensionless scattering phase space volume  $(P_3)[36]$  of (aoo) and (ooo) processes (where 'a' and 'o' indicate acoustic and optical phonons, respectively) of BC8-Si is tiny, indicating that the acoustic phonon scattering is significantly suppressed by the acoustic phonon dispersion. However, the (aoo) and (ooo) processes dominate phonon scattering processes in BC8-Si, contributing to the total phase space  $P_3$ . The former mostly stems from the phonon scattering between the acoustic phonons and low-lying optical branches, which forms a series of "flat bands" between 10 and 20 meV. The large phase space of (ooo) processes mostly results from the unique optical phonon branches of BC8-Si, in which the "flat" branches between 30 and 40 meV play a role of a "bridge" to provide more phonon scattering channels for the low energy optical phonons below 20 meV and high energy optical phonon beyond 50 meV. Therefore, the "flat optical bands" not only enhance the phonon-phonon scattering between acoustic and low-energy optical phonons, but also act as a scattering bridge between the high- and low-energy optical phonons. This enlarged scattering space greatly enhances the phonon-phonon scattering rate in BC8-Si and reduce its lattice thermal conductivity significantly.

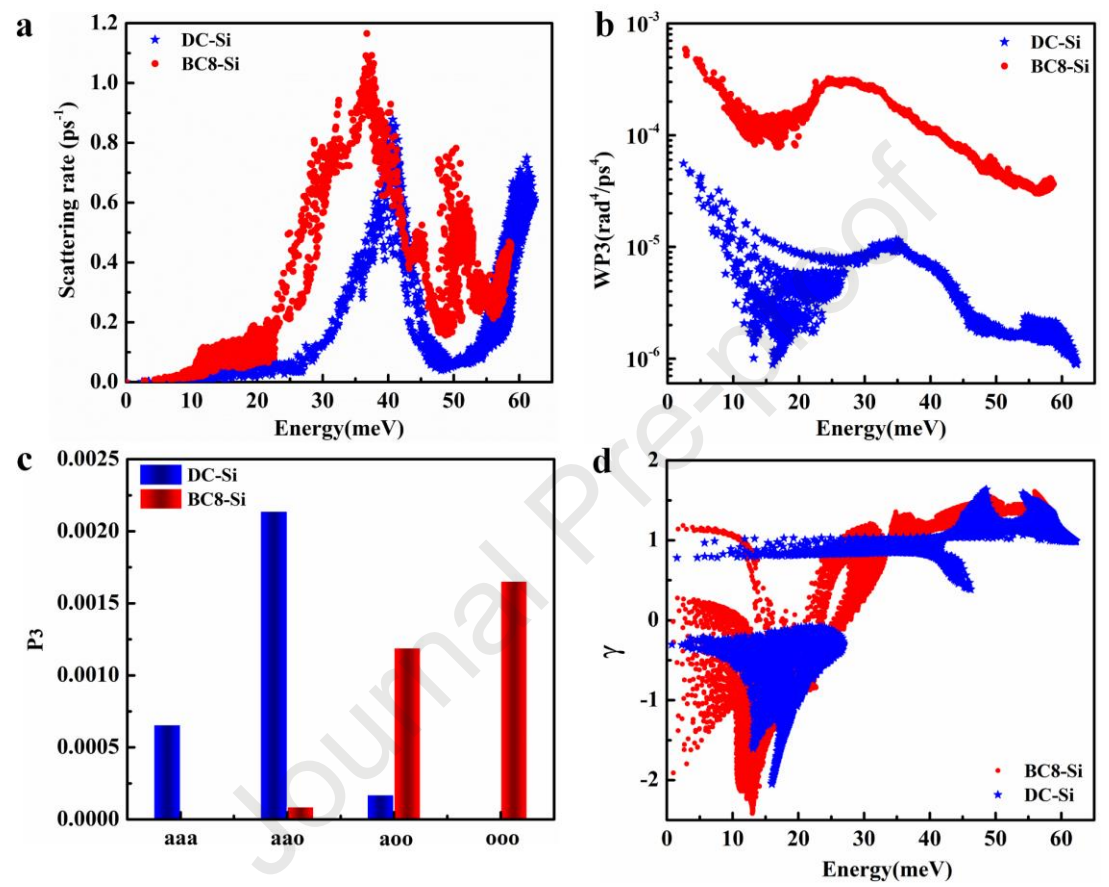


**Fig. 4.** Thermal transport properties for DC-Si and BC8-Si. Energy dependent (a) total scattering rates, (b) total weighted phase space at room temperature; (c) contribution of three-phonon scattering processes to total scattering phase-space volume, these processes are labeled as (aaa), (aao), (aoo) and (ooo), (d) energy dependent mode Grüneisen parameters.

#### 4. Conclusion

In summary, by combining experimental INS measurements and first-principles calculations based on the Boltzmann transport theory, the origin of the remarkable difference between lattice thermal conductivity of DC and BC8 silicon is revealed to be the dramatically larger phonon scattering phase space of BC8-Si. The "flat" optical phonon bands contribute to this large scattering phase space. Such bands between 10 and 20 meV enhance the scattering between acoustic and low energy optical phonons, while the bands between 30 and 40 meV act

as a scattering bridge between the high- and low-energy optical phonons. These findings provide the microscopic origin of the outstanding difference of thermal properties in DC-Si and BC8-Si, and provide insights for novel silicon allotropes and their development as efficient electronic device.

## Acknowledgments

This work is supported by the National Science Foundation of China (Grant No. 1217021241), Beijing Natural Science Foundation, China (Grant No. Z190011). CL acknowledges support by the National Science Foundation under Grant No. 1750786. TAS acknowledges support from NSF-DMR under Grant No. 1809756. This research used resources at the Spallation Neutron Source, a DOE Office of Science User Facility operated by the Oak Ridge National Laboratory. Theoretical calculations were performed using resources of the National Supercomputer Centre in Guangzhou.

## **Declaration of competing interest**

The authors declare that they have no known competing financial interests or personal relationships that could have appeared to influence the work reported in this paper.

## References

- [1] L. Rapp, B. Haberl, C.J. Pickard, J.E. Bradby, E.G. Gamaly, J.S. Williams, A.V. Rode, Experimental evidence of new tetragonal polymorphs of silicon formed through ultrafast laser-induced confined microexplosion, Nat Commun. 6 (2015) 7555. https://doi.org/10.1038/ncomms8555.
- [2] D.Y. Kim, S. Stefanoski, O.O. Kurakevych, T.A. Strobel, Synthesis of an open-framework allotrope of silicon, Nature Mater. 14 (2015) 169–173. https://doi.org/10.1038/nmat4140.
- [3] C. Lin, X. Liu, D. Yang, X. Li, J.S. Smith, B. Wang, H. Dong, S. Li, W. Yang, J.S. Tse, Temperature- and Rate-Dependent Pathways in Formation of Metastable Silicon Phases under Rapid Decompression, Phys. Rev. Lett. 125 (2020) 155702. https://doi.org/10.1103/PhysRevLett.125.155702.
- [4] Jamieson John C., Crystal Structures at High Pressures of Metallic Modifications of

- Silicon and Germanium, Science. 139 (1963) 762–764. https://doi.org/10.1126/science.139.3556.762.
- [5] H. Olijnyk, S.K. Sikka, W.B. Holzapfel, Structural phase transitions in Si and Ge under pressures up to 50 GPa, Physics Letters A. 103 (1984) 137–140. https://doi.org/10.1016/0375-9601(84)90219-6.
- [6] M. Hanfland, U. Schwarz, K. Syassen, K. Takemura, Crystal Structure of the High-Pressure Phase Silicon VI, Phys. Rev. Lett. 82 (1999) 1197–1200. https://doi.org/10.1103/PhysRevLett.82.1197.
- [7] Y.-X. Zhao, F. Buehler, J.R. Sites, I.L. Spain, New metastable phases of silicon, Solid State Communications. 59 (1986) 679–682. https://doi.org/10.1016/0038-1098(86)90372-8.
- [8] S.J. Duclos, Y.K. Vohra, A.L. Ruoff, Experimental study of the crystal stability and equation of state of Si to 248 GPa, Phys. Rev. B. 41 (1990) 12021–12028. https://doi.org/10.1103/PhysRevB.41.12021.
- [9] M.I. McMahon, R.J. Nelmes, New high-pressure phase of Si, Phys. Rev. B. 47 (1993) 8337–8340. https://doi.org/10.1103/PhysRevB.47.8337.
- [10] M.I. McMahon, R.J. Nelmes, N.G. Wright, D.R. Allan, Pressure dependence of the *Imma* phase of silicon, Phys. Rev. B. 50 (1994) 739–743. https://doi.org/10.1103/PhysRevB.50.739.
- [11] G. Weill, J.L. Mansot, G. Sagon, C. Carlone, J.M. Besson, Characterisation of Si III and Si IV, metastable forms of silicon at ambient pressure, Semicond. Sci. Technol. 4 (1989) 280–282. https://doi.org/10.1088/0268-1242/4/4/029.
- [12] H. Zhang, H. Liu, K. Wei, O.O. Kurakevych, Y. Le Godec, Z. Liu, J. Martin, M. Guerrette, G.S. Nolas, T.A. Strobel, BC8 Silicon (Si-III) is a Narrow-Gap Semiconductor, Phys. Rev. Lett. 118 (2017) 146601. https://doi.org/10.1103/PhysRevLett.118.146601.
- [13]S. Minomura, H.G. Drickamer, Pressure induced phase transitions in silicon, germanium and some III–V compounds, Journal of Physics and Chemistry of Solids. 23 (1962) 451–456. https://doi.org/10.1016/0022-3697(62)90085-9.
- [14] Wentorf R. H., Kasper J. S., Two New Forms of Silicon, Science. 139 (1963) 338–339. https://doi.org/10.1126/science.139.3552.338-b.
- [15] Kasper John S., Hagenmuller Paul, Pouchard Michel, Cros Christian, Clathrate Structure of Silicon Na8Si46 and NaxSi136 (x < 11), Science. 150 (1965) 1713–1714.

- https://doi.org/10.1126/science.150.3704.1713.
- [16] Q. Wang, B. Xu, J. Sun, H. Liu, Z. Zhao, D. Yu, C. Fan, J. He, Direct Band Gap Silicon Allotropes, J. Am. Chem. Soc. 136 (2014) 9826–9829. https://doi.org/10.1021/ja5035792.
- [17] Y. Guo, Q. Wang, Y. Kawazoe, P. Jena, A New Silicon Phase with Direct Band Gap and Novel Optoelectronic Properties, Sci Rep. 5 (2015) 14342. https://doi.org/10.1038/srep14342.
- [18] K. Chae, S.-H. Kang, S.-M. Choi, D.Y. Kim, Y.-W. Son, Enhanced Thermoelectric Properties in a New Silicon Crystal Si <sub>24</sub> with Intrinsic Nanoscale Porous Structure, Nano Lett. 18 (2018) 4748–4754. https://doi.org/10.1021/acs.nanolett.8b01176.
- [19] C. Bai, C. Chai, Q. Fan, Y. Liu, Y. Yang, Correction: A Novel Silicon Allotrope in the Monoclinic Phase. Materials 2017, 10, 441, Materials. 10 (2017). https://doi.org/10.3390/ma10050561.
- [20] V.E. Dmitrienko, V.A. Chizhikov, Infinite family of b c 8 -like metastable phases in silicon, Phys. Rev. B. 101 (2020) 245203. https://doi.org/10.1103/PhysRevB.101.245203.
- [21] O.O. Kurakevych, Y. Le Godec, W.A. Crichton, J. Guignard, T.A. Strobel, H. Zhang, H. Liu, C. Coelho Diogo, A. Polian, N. Menguy, S.J. Juhl, C. Gervais, Synthesis of Bulk BC8 Silicon Allotrope by Direct Transformation and Reduced-Pressure Chemical Pathways, Inorg. Chem. 55 (2016) 8943–8950. https://doi.org/10.1021/acs.inorgchem.6b01443.
- [22] J.Y.Y. Lin, A. Banerjee, F. Islam, M.D. Le, D.L. Abernathy, Energy dependence of the flux and elastic resolution for the ARCS neutron spectrometer, Physica B: Condensed Matter. 562 (2019) 26–30. https://doi.org/10.1016/j.physb.2018.11.027.
- [23] J. Taylor, O. Arnold, J. Bilheaux, A. Buts, S. Campbell, M. Doucet, N. Draper, R. Fowler, M. Gigg, V. Lynch, Mantid, a high performance framework for reduction and analysis of neutron scattering data, in: 2012: pp. W26-010.
- [24] M. Kresch, O. Delaire, R. Stevens, J.Y.Y. Lin, B. Fultz, Neutron scattering measurements of phonons in nickel at elevated temperatures, Phys. Rev. B. 75 (2007) 104301. https://doi.org/10.1103/PhysRevB.75.104301.
- [25]O. Delaire, M. Kresch, J.A. Muñoz, M.S. Lucas, J.Y.Y. Lin, B. Fultz, Electron-phonon interactions and high-temperature thermodynamics of vanadium and its alloys, Phys. Rev. B. 77 (2008) 214112. https://doi.org/10.1103/PhysRevB.77.214112.
- [26] P.E. Blöchl, Projector augmented-wave method, Phys. Rev. B. 50 (1994) 17953–17979.

- https://doi.org/10.1103/PhysRevB.50.17953.
- [27]G. Kresse, J. Furthmüller, Efficiency of ab-initio total energy calculations for metals and semiconductors using a plane-wave basis set, Computational Materials Science. 6 (1996) 15–50. https://doi.org/10.1016/0927-0256(96)00008-0.
- [28] J.P. Perdew, K. Burke, M. Ernzerhof, Generalized Gradient Approximation Made Simple, Phys. Rev. Lett. 77 (1996) 3865–3868. https://doi.org/10.1103/PhysRevLett.77.3865.
- [29] P.E. Blöchl, O. Jepsen, O.K. Andersen, Improved tetrahedron method for Brillouin-zone integrations, Phys. Rev. B. 49 (1994) 16223–16233. https://doi.org/10.1103/PhysRevB.49.16223.
- [30] A. Togo, I. Tanaka, First principles phonon calculations in materials science, Scripta Materialia. 108 (2015) 1–5. https://doi.org/10.1016/j.scriptamat.2015.07.021.
- [31] W. Li, J. Carrete, N. A. Katcho, N. Mingo, ShengBTE: A solver of the Boltzmann transport equation for phonons, Computer Physics Communications. 185 (2014) 1747–1758. https://doi.org/10.1016/j.cpc.2014.02.015.
- [32]G. Nilsson, G. Nelin, Study of the Homology between Silicon and Germanium by Thermal-Neutron Spectrometry, Phys. Rev. B. 6 (1972) 3777–3786. https://doi.org/10.1103/PhysRevB.6.3777.
- [33] E.S. Toberer, A. Zevalkink, G.J. Snyder, Phonon engineering through crystal chemistry, J. Mater. Chem. 21 (2011) 15843. https://doi.org/10.1039/c1jm11754h.
- [34] W. Li, N. Mingo, Thermal conductivity of fully filled skutterudites: Role of the filler, Phys. Rev. B. 89 (2014) 184304. https://doi.org/10.1103/PhysRevB.89.184304.
- [35] W. Li, N. Mingo, Ultralow lattice thermal conductivity of the fully filled skutterudite YbFe 4 Sb 12 due to the flat avoided-crossing filler modes, Phys. Rev. B. 91 (2015) 144304. https://doi.org/10.1103/PhysRevB.91.144304.
- [36] L. Lindsay, D.A. Broido, Three-phonon phase space and lattice thermal conductivity in semiconductors, J. Phys.: Condens. Matter. 20 (2008) 165209. https://doi.org/10.1088/0953-8984/20/16/165209.

John Million Control

# **Highlights**

- BC8 silicon not only has a narrow-band gap, but also unusually low thermal conductivity, i.e., 1-2 orders of magnitude lower than that of DC-Si, although they have similar cubic structure and very close Si-Si bond lengths.
- Combining the inelastic neutron scattering (INS) and the first-principles calculations, the primary origin of the strikingly different thermal conductivity of BC8-Si and DC-Si is revealed.
- Flat phonon bands are found to play critical role in the reduction of lattice thermal conductivity in BC8-Si. Such bands in the high energy range act as a *scattering bridge* between the high energy optical phonons and other low energy phonons.

## **Declaration of competing interest**

The authors declare that they have no known competing financial interests or personal relationships that could have appeared to influence the work reported in this paper.